

**Title:**

A Mesh Generation Methodology for Laser Cladding Models with Variable Overlapping Beads

Authors:

Parvaneh Zareh, zareh@uwindsor.ca, University of Windsor

Ruth Jill Urbanic, jurbanic@uwindsor.ca, University of Windsor

Keywords:

Metal Additive Manufacturing, Finite Element Modeling Geometric Based Interpretation, Bead Overlap Variations, Heat Source, Mesh Development

DOI: 10.14733/cadconfP.2019.273-277

Introduction:

The co-axial laser cladding process is a surface modification process that deposits a material onto a substrate. It offers some distinct advantages for surface characteristics modification when compared to thermal spray and welding, as the heat source is focused, resulting in good control of the depth of the dilution zone (bonding region between the clad and the substrate). Materials with the desired mechanical and physical properties are used to coat surfaces, or to refurbish worn-out surfaces. The laser beam melts a thin layer of the substrate surface to create metallurgical bond between the coating material and work-piece [2, 3, 6]. In the laser cladding process, the laser beam acts as a heat source to melt the coating material powder while it is deposited onto the substrate surface. The process for this research uses a coaxial nozzle to inject the powder into the melt pool on the substrate. Each input parameter (laser power, travel speed, powder feed rate, contact tip to work piece distance) affects the bead's mechanical and physical properties. It is crucial to find the best combination of input parameters to deposit a bead with both the desired geometry and mechanical properties. For a better understanding of the laser cladding process, and to explore 'what if' strategies, a simulation model, such as a finite element model, can be employed. To attain accurate numerical results, the generation of a representative geometric model and a high-quality mesh is essential.

The geometry of the coating layer changes based on the toolpath for the heat source. There will be overlap regions, and the amount of overlap depends on the geometry and process planner's settings. Variable overlap conditions typically occur at a boundary region. As shown in Fig. 1 (a) for a tool path of a layer for a cylinder there are three different overlap scenarios, and in Fig. 1 (b), two different overlap scenarios are shown for the star shape. For both examples, the default 'side to side' overlap is 50%, but it can reach 75%, and the 'raster fill to boundary pass' overlap is 50%. The long-term goal of this research is to understand the consequences of a variable overlap condition on the beads' mechanical and physical properties. This research is relevant for laser cladding a surface, and metal additive manufacturing, where a direct energy deposition process is employed to fabricate a near net shape model.

Initial research is being conducted for a controlled overlap experiment, as shown in Fig. 2. Here a layer of AISI 420 is deposited onto a mild steel plate (5 mm thick, and 30 mm wide). The plate is 100 mm long, and the bead length is 80 mm. The bead overlap percentages are 30% and 50%, respectively for 10 mm of travel at the beginning and the end of the deposition. The overlap varies from 30% to 50% for 60 mm between these two constant overlap areas. Two multi-track bead scenarios were considered: a two-bead and a four-bead setting. The immediate research goal is to develop an experimentally calibrated simulation model to explore the influence of the percentage overlap on the deposited beads' physical and mechanical properties.

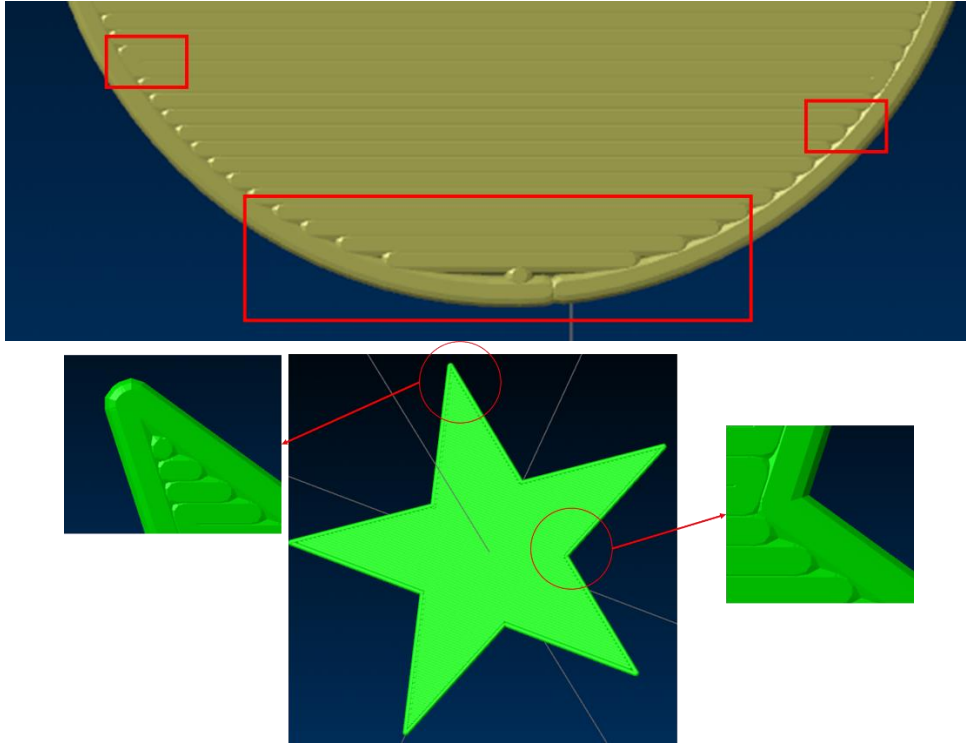


Fig. 1: (a) A layer slice for a cylinder and its bead deposition geometry, (b) a layer slice for a star and its bead deposition geometry.

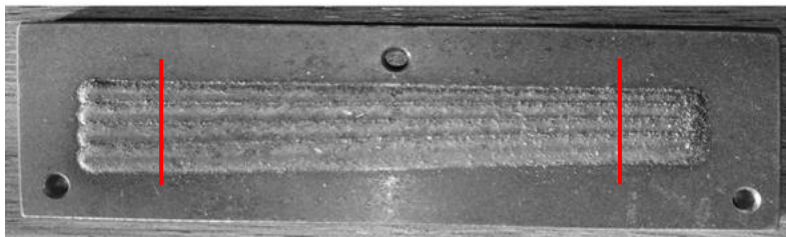
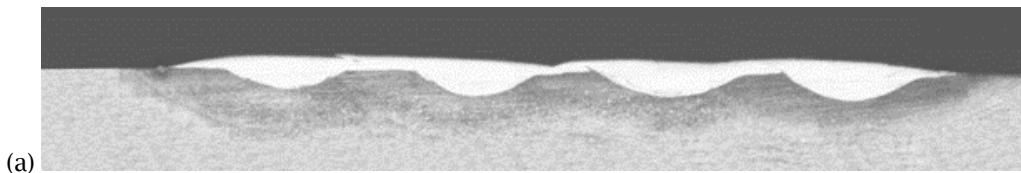


Fig. 2: A layer of deposited clad beads with the overlap percentage varying from 30% to 50%.

For generating the sample shown in Fig. 2, a 2.4 kW laser beam travelled along the substrate at a speed of 15 mm/s. The powder feed rate was 19 g/sec, the contact tip to work piece distance was 23 mm, and the focal length setting was 400 mm. A 'one-way' travel path strategy was utilized. Fig. 3 shows the cross-section view of the sample (Fig. 2) at the beginning (30% overlap) and at the end (50% overlap).



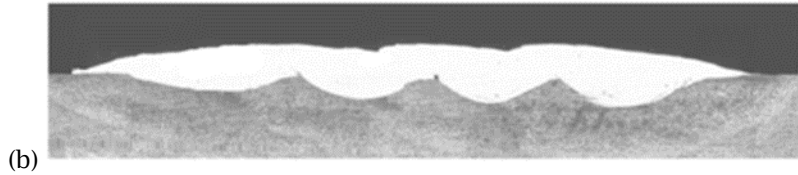


Fig. 3: Cross-section of sample at: a) the end of the 30% overlap, b) the beginning of the 50% overlap.

Some researchers [1, 2, 4, 5] have generated finite elements models for multi-track beads with a constant overlap percentage between the two adjacent beads. In their models with constant overlap percentages, the height of the beads remains constant from the beginning to the end of the deposition, the beads are parallel to the plate edge, and the contact surface between each two beads is a constant planar surface. For the case with the beads with a variable overlap percentage, not only does the height of the beads change along the deposition path (by approximately 25%), but the contact surface between each two adjacent beads is not constant. Additionally, the raster angles of the beads to the edges vary for each bead except in the 10 mm constant overlap regions. Based on these reasons, the geometric models are highly unstructured and a structured mesh cannot be readily generated employing standard tools.

<i>Geometry Measurements</i>								
Bead No.	<i>Height of the beads (mm)</i>				<i>Width of the beads (mm)</i>			
	B1	B2	B3	B4	B1	B2	B3	B4
30% Cross-section	0.4	0.405	0.41	0.412	4.11	3.9	3.8	3.7
50% Cross-section	0.503	0.514	0.519	0.522	3.06	2.37	2.41	2.62

Tab. 1: The bead geometry values used for generating the model.

Main idea:

A structured mesh needs to be developed for the simulation models. One way to generate a structured mesh for this unstructured geometry is to divide it into sub-segments. The main point which should be noted with this dividing process is that each area for one bead should be connected to **only** one area on another bead. As it can be seen in Table 1, the height increases during the deposition and the visible width of the deposited material decreases. This fact, along with having variations in the contact surfaces, makes the CAD model generation complicated. One solution that was investigated was using the multi-section command in the CAD software. Fig. 4 shows two clad beads which were generated with the multi-section command in CATIA[®].

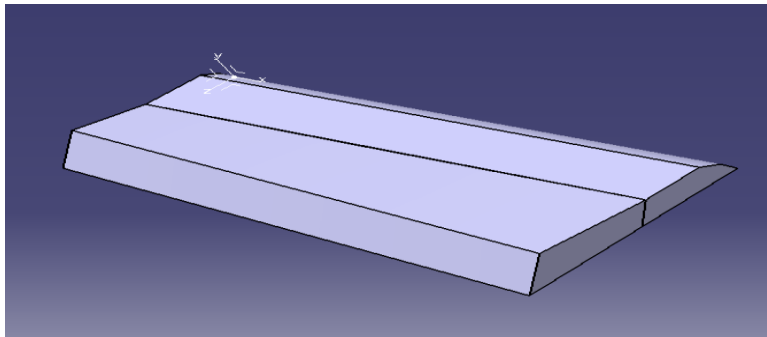


Fig. 4: The geometric model of two clad beads illustrating the variable overlap regions.

When importing the geometric model (shown in Fig. 4) into a finite element software solution (ANSYS®) and activating the structured mesh command, an error message indicated that this model could not be used for the generation of a mapped mesh. Fig. 5 shows the cross-section of the 2 beads shown in Fig. 4. As it can be seen, the contact areas of the first bead and the second bead are not connected to each other – there is a gap.

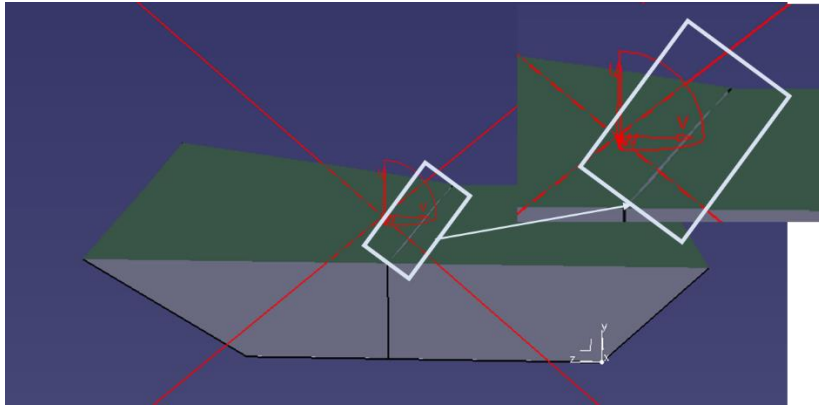


Fig. 5: The cross-section of two beads shown in Fig. 3.

One solution alternative performed by Nazemi and Urbanic [5] was to activate bricks to address the corner and changes in the contact surface for a spiral toolpath (inside – out deposition pattern). This can be seen in Fig. 6. It was time consuming to generate the mesh for this simulation, and this solution approach was problematic for the variable overlapping bead geometry.

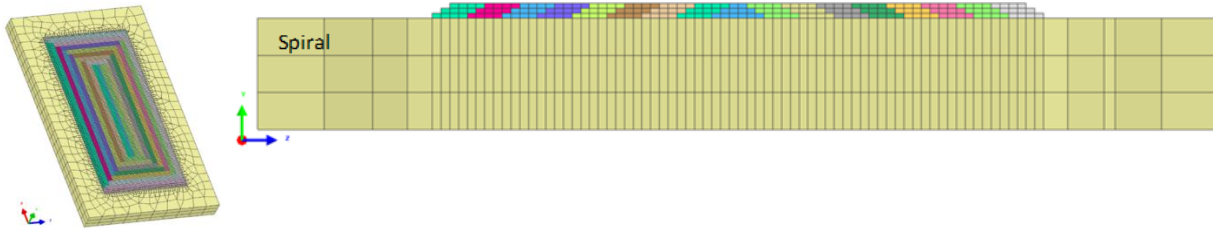


Fig. 6: (a) A spiral inside to out tool path with constant overlap, and (b) brick elements to model the elements, adapted from [5].

As shown in Fig. 7 this study introduces a solution for generating a mapped mesh for this unstructured geometry. A procedure for dividing the deposition area is described, and will be expanded upon for curvilinear scenarios. All the small volumes should overlay each other and the distance between their adjacent areas cannot be more than more than 1×10^{-8} mm to be useable for structured mapped mesh generation. The two bead and four bead geometric models were divided into 214, and 278 small pieces, respectively.

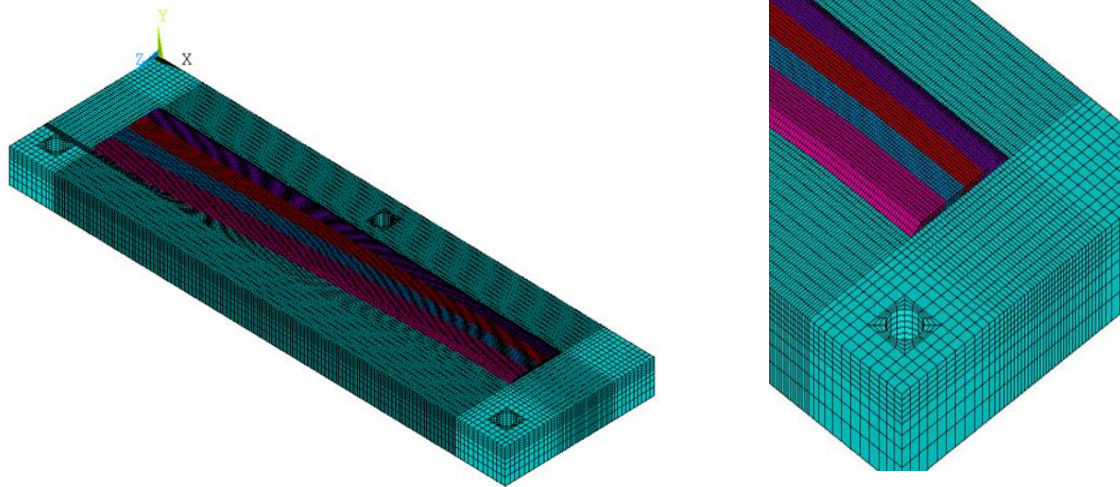


Fig. 7: The brick mesh generated for the geometric models shown in Fig. 2.

Conclusion:

To model the laser cladding process a 3D thermo-mechanical FE model was developed. When laser cladding, a laser beam with a small spot area moves across a surface melting the substrate and the deposited powder. A large amount of energy is transferred into substrate over a short time period, and the FE model for this process is complex. The heat transfer model included the convective heat transfer of the fluid flow inside the melt-pool, called the “thermocapillary (Marangoni) flow,” and the physical and material properties vary based on the temperature. Adding to the model’s complexity is the physical bead configuration being investigated. The variable overlap condition introduced variable bead geometry, and a double angle geometry configuration for the bead. Development of a structured mesh proved challenging. The quality of the mesh affects the convergence of the numerical model, the accuracy of the results, and the computation time; consequently, a methodology to divide and link segments is developed. Based on the node number limitations in the FE software, and the fact that a mapped mesh uses lower number of nodes, this mesh helps to save nodes in non-critical areas and enables a more refined mesh to be used the areas which touch the heat source directly.

References:

- [1] Chew, Y.; Pang, J.; Bi, G.; Song, B.: Thermo-mechanical model for simulating laser cladding induced residual stresses with single and multiple clad beads, *Journal of Materials Processing Technology*, 224, 2015, 89-101. <https://doi.org/10.1016/j.jmatprotec.2015.04.031>
- [2] Farahmand, P.; Kovacevic, R.: An experimental-numerical investigation of heat distribution and stress field in single- and multi-track laser cladding by a high-power direct diode laser, *Optics & Laser Technology*, 63, 2014, 154-168. <https://doi.org/10.1016/j.optlastec.2014.04.016>
- [3] Komvopoulos, K.; Nagarathnam, K.: Processing and characterization of laser cladded coating materials, *Journal of Engineering Material Technology*, 112(2), 1990, 131-143. <https://doi.org/10.1115/1.2903299>
- [4] Nazemi, N.; Urbanic, R. J.; Alam, M.: Hardness and residual stress modeling of powder injection laser cladding of P420 coating on AISI 1018 substrate, *International Journal of Advanced Manufacturing Technology*, 93, 2017, 3485. <https://doi.org/10.1007/s00170-017-0760-9>
- [5] Nazemi, N.; Urbanic, R. J.: A numerical investigation for alternative toolpath deposition solutions for surface cladding of stainless steel P420 powder on AISI 1018 steel substrate, *International Journal of Advanced Manufacturing Technology*, 96(9-12), 2018, 4123-4143. <https://doi.org/10.1007/s00170-018-1840-1>
- [6] Shukla, M.; Verma, V.: Finite element simulation and analysis of laser metal deposition, 6th International Conference on Mechanical, Production & Automobile Engineering, 2014.